process wherein no electrons are ejected (indeed this assumption has been used above). However, when A is of the order of several hundred electron volts as it is for the more violent collisions, it seems unlikely that such a reaction could occur. Possibly the energy is consumed in some process such as Auger electron emission which occurs with high probability and which requires high and approximately constant energy for every charge state produced.

When the coefficients B and C exceed unity, the average inelastic energy asssociated with the removal of an electron exceeds that required spectroscopically. That is, the average energy associated with the removal of the $(n+1)$st electron is $C(U''_{n+1} - U''_n)$, and that not accounted for in ionization is $(C-1)(U''_{n+1} - U''_n)$. The problem of determining the manner in which this energy is consumed is indeterminate.

*Work sponsored by the U.S. Air Force Office of Scientific Research.

†Present address: Département de Physique, Université Laval, Québec 10e, Canada.

[1]E. J. Knystautas, Q. C. Kessel, R. Del Boca, and H. C. Hayden, Phys. Rev. A 1, 825 (1970).

[2]A. Russek and M. T. Thomas, Phys. Rev. 109, 2015 (1958).

[3]E. Everhart and Q. C. Kessel, Phys. Rev. 146, 27 (1966).

[4]W. F. van der Weg, D. J. Bierman, and D. Onderdelinden (unpublished).

[5]Q. C. Kessel, M. P. McCaughey, and E. Everhart, Phys. Rev. 153, 57 (1967).

[6]M. P. McCaughey, E. J. Knystautas, and E. Everhart, Phys. Rev. 175, 14 (1968).

[7]V. V. Afrosimov, Yu. S. Gordeev, A. M. Polyansky, and A. P. Shergin, *Sixth International Conference on the Physics of Electronic and Atomic Collisions, Abstracts of Papers* (MIT Press, Cambridge, Mass., 1969), p. 744.

[8]Q. C. Kessel and E. Everhart, Phys. Rev. 146, 16 (1966).

[9]W. Finkelnburg and W. Humbach, Naturwiss. 42, 36 (1955).

[10]A. G. Worthing and J. Geffner, *Treatment of Experimental Data* (Wiley, New York, 1943), Chaps. XI and XII.

PHYSICAL REVIEW A VOLUME 3, NUMBER 1 JANUARY 1971

Distributions in Energy and Angle of Electrons Ejected from Molecular Nitrogen by 0.3- to 1.7-MeV Protons*

L. H. Toburen
Battelle Memorial Institute, Pacific Northwest Laboratories, Richland, Washington 99352
(Received 14 May 1970)

Cross sections, differential in ejection energy and angle, for electron emission from nitrogen following proton impact were measured for protons with energies from 0.3 to 1.7 MeV. Electrons were detected at emission angles from 20° to 130° with energies from a few eV to approximately 4000 eV. Cross sections differential in energy were obtained from the doubly differential cross sections by integration with respect to the emission angle. These results were compared with cross sections calculated from binary-encounter theory. Agreement between the calculated and measured cross sections was within experimental uncertainties (25%) throughout most of the energy range of the ejected electrons. K-shell ionization cross sections for nitrogen were also estimated from the intensity of the K Auger electrons emitted following proton impact.

I. INTRODUCTION

Secondary electrons produced in ion-atom and ion-molecule reactions play an important role in atmospheric, plasma, and radiological physics. The study of the energy and angular distributions of electrons ejected by proton impact is a sensitive means of testing the theory of atomic and molecular collision processes. For collisions between incident protons and target atoms (or molecules) in which the energy transfer is large compared to the electron binding energies, gross features of the collision, such as the ionization cross sections, which are calculated from existing theory, agree well with experimental data. Calculations of more explicit descriptions of the collision process, however, such as the angular distribution of secondary electrons of a given ejection energy, may differ from measured values by more than an order of magnitude. These discrepancies indicate the need for more experimental and theoretical work.

Measurements of absolute cross sections, differential in both electron energy and emission angle, for electron ejection from gases following proton impact have been conducted by Kuyatt and Jorgensen,[1] Rudd and Jorgensen,[2] and Rudd, Sautter, and Bailey.[3] These measurements were limited to protons with energies from 50 to 300 keV and to hydrogen and helium as target gases. In the present work, we have measured absolute cross sections, differential in electron energy and emission angle, for ejection of electrons from molecular nitrogen by protons with energies between 0.3 and 1.7 MeV. Electron energy distributions were measured for emission angles from 20° to 130° with respect to the forward direction of the proton beam.

II. EXPERIMENTAL METHOD

A schematic drawing of the apparatus used to measure the energy and angular distributions is shown in Fig. 1. The proton beam was supplied by a Van de Graaff accelerator with a voltage range of 0.3 to 1.7 MeV, and was collimated to 0.34 mm in diameter by apertures 1 and 2 shown in Fig. 1. These two collimators were separated by approximately 50 cm in order to define a proton beam with a small angular divergence in the target region. Collimator 3, 0.76 mm in diameter, was maintained at − 67.5 V to suppress electrons which may have been produced by slit edge scattering. The potential on collimator 3 was shielded from the interaction region by collimator 4 which contained an aperture 1.52 mm in diameter. After the beam passed through the target cell, the protons were collected in a shielded Faraday cup. A biased collimator placed in front of the Faraday cup, but well within the electrostatic shield surrounding it, was held at − 67.5 V to prevent the escape of secondary electrons from the cup. The target gas cell, shown in Fig. 1, was fabricated in a shape approximately that of a wedge. The "point" of the wedge was machined to a cylindrical shape with a radius of 6.35 mm. A slit 0.64 mm wide was machined along the circumference of this cylindrical portion to allow the proton beam to pass through the target gas and to allow electrons produced within the cell to escape. This slit was cut slightly more than 180° around the cylinder in order to allow the proton beam to pass through the slit at a position along the diameter of the cylindrical portion of the cell. The target cell was designed with this shape to reduce the probability of electrons scattering from the back walls of the target cell and into the analyzer. As a further precaution against scattering, the back wall of the target cell was lined to approximately 1.0 cm thickness with crumpled 98% transmission mesh to act as a "sponge" to electrons. By high speed pumping of the volume surrounding the target cell, a pressure differential of approximately 100 was obtained between the interior of the target cell and the surrounding vacuum chamber. This pressure differential and the design of the target cell helped to reduce the probability that an electron ejected in the direction of the electrostatic analyzer would undergo a collision before it was detected.

The electrostatic analyzer used for the measurements of the electron energy distributions is of the cylindrical mirror type and has been described by several authors.[4-6] In our work, the electrostatic analyzer was collimated to an angular acceptance of approximately 5.5°. The energy resolution of the analyzer was determined from measurements of the shape of the K and L Auger lines of nitrogen and argon, respectively. The resolution obtained

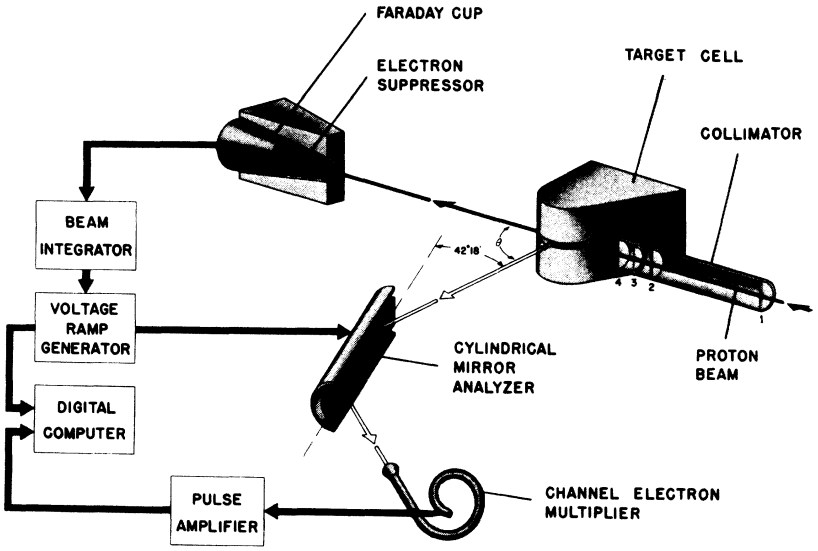

FIG. 1. Schematic drawing of the apparatus used for the cross-section measurements.

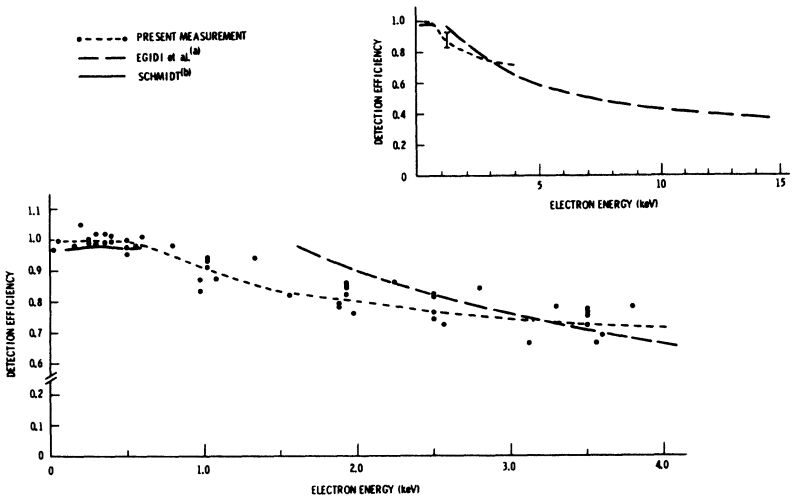

FIG. 2. Detection efficiency for the continuous channel electron multiplier. Previous measurements: (a) see Ref. 7; (b) see Ref. 8.

in this way agreed well with the calculated value of 5.5% full width at half-maximum (FWHM). Dimensions for the electrostatic analyzer were chosen to make the energy of the transmitted electrons, in electron volts, nearly equal to the potential, in volts, applied to the analyzer. After the electrons were energy analyzed, they were detected by a continuous channel electron multiplier operated in a space-charge saturated mode. The detection efficiency of the electron multiplier, defined as the ratio of the number of output pulses to the number of incident electrons, is shown in Fig. 2. An absolute detection efficiency of 0.98 ± 0.04 for 500- to 600-eV electrons was obtained for our continuous channel electron multiplier by comparing it to a windowless geiger counter. The detection efficiency at other electron energies was determined relative to this value by means of an electron gun which provided electron intensities independent of the acceleration potential. The best fit to our results, indicated by the dashed line in Fig. 2, is in agreement with previous measurements[7,8] at both the high-energy and low-energy extremes of our investigation and has been assigned an uncertainty of $\pm 5\%$ with confidence limits of 1 standard deviation.

The gas density in the differentially pumped target cell was maintained constant by means of an automatic pressure controller coupled to a capacitance manometer which continuously monitored the pressure in a gas reservoir below the target cell. The gas density in the center of the target cell was then deduced from this pressure measurement. Since the target cell and gas reservoir were separated by approximately 20 cm, it was necessary to determine the extent of the pressure differential between these two regions due to the conductance of the transfer tube between them. For the purpose of this measurement, a second capacitance manometer was used to measure directly the gas pressure in the target cell. From simultaneous measurements of the target cell and reservoir gas pressures, it was found that the target cell pressure was 62% of the corresponding value measured for the gas reservoir. The pressure differential determined by these measurements was in close agreement with the value calculated using the equations of Dushman.[9]

Magnetic fields in the vicinity of the interaction region were reduced to a few milligauss by means of three mutually perpendicular pairs of 7-ft, square Helmholtz coils. Reduction of the residual magnetic field to this level provided assurance that the trajectories of electrons with energies of more than a few eV were not significantly altered prior to their energy analysis and detection. The vertical component of the magnetic field near the interaction region was monitored continuously during data accumulation and the lateral components were checked periodically to ensure optimum field nullification.

All collimators which define the proton and electron trajectories were machined to have thin edges to reduce slit edge scattering, and all voltages supplied to the system were electrostatically shielded from the interaction region.

III. DATA REDUCTION AND ERROR ANALYSIS

The basic features of the data handling system are indicated in Fig. 1. The electron energy distributions were obtained, for a given proton energy and angle of electron ejection, by counting the number of electrons transmitted by the electrostatic analyzer at a given voltage setting while a preset number of protons passed through the target cell. The proton current was monitored by an electrometer and integrated by a voltage-to-fre-

quency converter and scaler. After a preset number of protons were collected, the voltage on the electrostatic analyzer was automatically stepped and the integration process repeated. The number of electrons collected during a proton integration time was recorded in the multichannel analyzer operated as a multiscaler at a channel location determined by the voltage on the electrostatic analyzer. These data were then punched on IBM cards and transmitted to a digital computer for cross-section calculations. The cross sections, differential in observation angle θ and the electron energy ϵ, were calculated from the following equation:

$$\sigma(\theta, \epsilon) = \frac{N_e e^{\alpha P x}}{N_p P \, dS \Delta E \, 3.23 \times 10^{16}} \text{ cm}^2/\text{eV sr molecule} , \quad (1)$$

where N_e is the number of electrons counted while a number of protons N_p passed through the target cell; P is the target gas pressure in Torr; ΔE is the energy spread of the electrons transmitted by the analyzer; dS is the product of solid angle subtended by the analyzer and the proton path length observed within this solid angle; α is the absorption coefficient for electrons of energy ϵ in the target gas; and x is the effective path length of the electrons through the target gas including the effects of differentially pumping the target cell. The spread in electron energies transmitted by the electrostatic analyzer ΔE was obtained as the product of the analyzer resolution (5.5% FWHM) and the mean electron energy ϵ transmitted at each voltage setting. A modified form of the program of Bar-Avraham and Lee[10] for calculation of solid angles was applied to calculate dS. This quantity was obtained by calculating the differential solid angle $d\Omega$ subtended at the analyzer by each element of path length dl along the proton track and then integrating with respect to dl. The incremental values $d\Omega dl$ were evaluated from the characteristics of the analyzer collimation which included the aperture sizes, distances between the apertures and the proton beam, and the angle between the collimation axis of the electrostatic analyzer and the proton beam. The length of proton path subtended by the analyzer was, for angles other than 90°, longer than the diameter of our target cell. The target density is therefore not constant along the entire length of the proton path from which electrons could be accepted by the electrostatic analyzer. In order to account for this density variation, an additional program was written to calculate the density distribution of target gas molecules along the proton track as a function of the distance from the center of the target cell. This calculation, based on molecular flow of gas out of the differentially pumped slit in the target cell, was used to weight each incremental solid angle $d\Omega dl$ according to the gas density at the point along the proton track at which the increment was evaluated. The correction to the value of dS due to the variation in gas density along the proton track varied from 3% at 90° to 36% at 20°. A check on the accuracy of this calculation was made by measuring the angular distribution of K Auger electrons from nitrogen. Since these electrons originate from an initial S vacancy ($l = 0$), an isotropic distribution is expected. In Fig. 3, the cross sections for K Auger emission from nitrogen are plotted as a function of emission angle for 1.4- and 1.7-MeV proton impact. These cross sections were obtained by first subtracting an interpolated curve representing the contribution due to electrons ejected by direct interactions from the complete curve in the region of the Auger group and then integrating this result with respect to electron energy. The fact that the angular distribution of K Auger electrons thus obtained is isotropic (the dashed line in Fig. 3 has zero slope as implied by an isotropic distribution) indicates not only that the correction for the variation in density along the proton track observed by the analyzer was necessary, but also that the correction made was valid. The uncertainty in the absolute value calculated for the integral of the product of solid angle and path length, dS, based on uncertainties in the correction for variations in density along the proton track and uncertainties in the dimensions and positions of the collimators was estimated as 10%.

The term $e^{\alpha P x}$ in Eq. (1) corrects for the absorption of electrons in the target gas. Absorption coefficients α for electrons in nitrogen and hydrogen were taken from the work of Normand.[11] An effective absorption length x was deduced from the gas density distributions calculated above. The value of x also includes the path length through the electrostatic analyzer weighted according to the

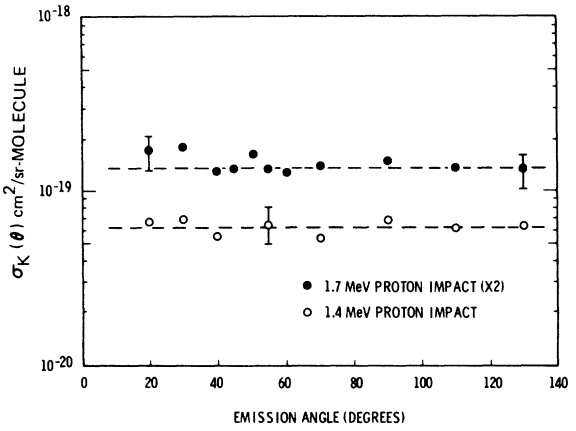

FIG. 3. Angular distribution of K Auger electrons from nitrogen for 1.4- and 1.7-MeV proton impact.

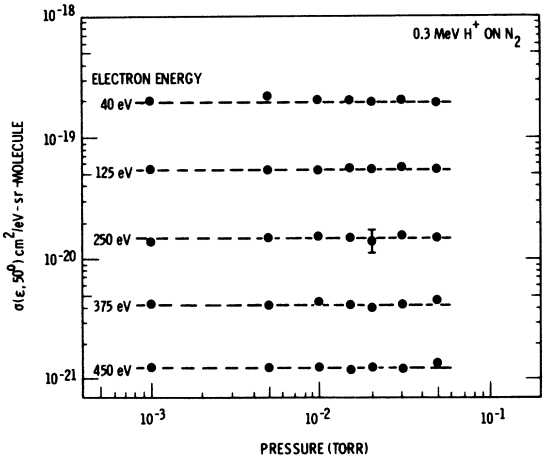

FIG. 4. Cross sections for electron emission as a function of target gas pressure for several electron energies. The electron emission angle was 50° and the proton energy was 0.3 MeV.

density of gas in that region. In order to assure that the cross sections were measured under single collision conditions and that proper account was taken of the absorption of electrons in the target gas, a study of the dependence of the cross sections on target pressure was made. The results of this investigation for 0.3-MeV protons on nitrogen, shown in Fig. 4, clearly indicate that the measured cross sections are independent of pressure. A similar investigation for 0.3-MeV protons on hydrogen gas gave results which also were independent of pressure. A target pressure of 0.0062 Torr was used for the measurements reported in this paper. The uncertainty in the density of the target gas due to uncertainties in the measurement of the target gas pressure was estimated to be 10%.

The combined systems for integration of the proton beam current and for automatic advancement of the analyzer voltage were calibrated to ± 5% by means of a standard current source. This calibration was checked before and after each energy scan of an electron spectrum to determine if any drifts in the voltage biases occurred during the run. Scans took typically three hours to complete. Data points were obtained at 2-eV intervals with approximately 10^{12} protons collected at each point. At higher electron energies, where the spread in electron energies transmitted by the analyzer was much greater than 2 eV, several data points were averaged together when the cross sections were calculated in order to improve the statistical significance of the results.

The total uncertainty in the measured cross sections is a combination of the statistical uncertainties associated with the determination of gas density, solid angle, etc. The uncertainty in the absolute value of the cross sections was estimated as the square root of the sum of the squares of the uncertainties associated with the determinations of target gas density, the product of solid angle and path length, ion-charge collection efficiency, analyzer resolution, the correction for electron absorption, and the electron detection efficiency. An estimated uncertainty of 25% in the absolute value of the cross sections was obtained by the above method. The contribution to the total uncertainty in the measured cross sections due to statistical effects of counting electrons varies from less than 1% for high count rates (low-energy electrons) to 50%, or possibly more, where the electron count rate is comparable to the background (high-energy electrons). Representative error bars indicative of the total uncertainties in the measured cross sections are shown in the figures in which the results are reported. The reproducibility of the data was tested by repeated scans over electron energy for several protons energies and for several electron ejection angles. These results were obtained over a period of several months during which the apparatus had been disassembled several times. Data obtained in these repeated scans yielded cross sections which were in agreement to within approximately 10%.

The uncertainty in the measured electron energies was estimated to be 2% based on an energy calibration of the electrostatic analyzer by means of an electron gun and by measurements of the energy of the $2p$-$3p3p$ Auger line of argon at 206 ± 2 eV[12] and the $KL_{2,3}L_{2,3}$ lines of neon at 805 ± 0.5 eV.[13]

IV. EXPERIMENTAL RESULTS

In order to check the agreement between our measurements and the results of previous work, we measured cross sections for electron emission from the molecular hydrogen for 0.3-MeV proton impact. These cross sections, differential in electron emission energy and angle, are compared to the measurements of Rudd *et al.*[3] in Fig. 5. In most cases, the cross sections reported in this paper were multiplied by the respective electron energy before being plotted in order to reduce the number of orders of magnitude necessary to display the results. It is expected that this method of presenting the results will improve the accuracy with which one can read numerical values from the graphs.[14] Plotted in this form, the curves represent cross sections for the transfer of a given amount of kinetic energy ϵ to a bound electron such that the ejected electron moves in a specified direction θ with respect to the proton beam. Agreement between the results of the present measurements and those of Rudd *et al.*[3] is extremely good with the exception of the low-energy end of the spectra for electron emission at 30°, 50°, and 70°. For elec-

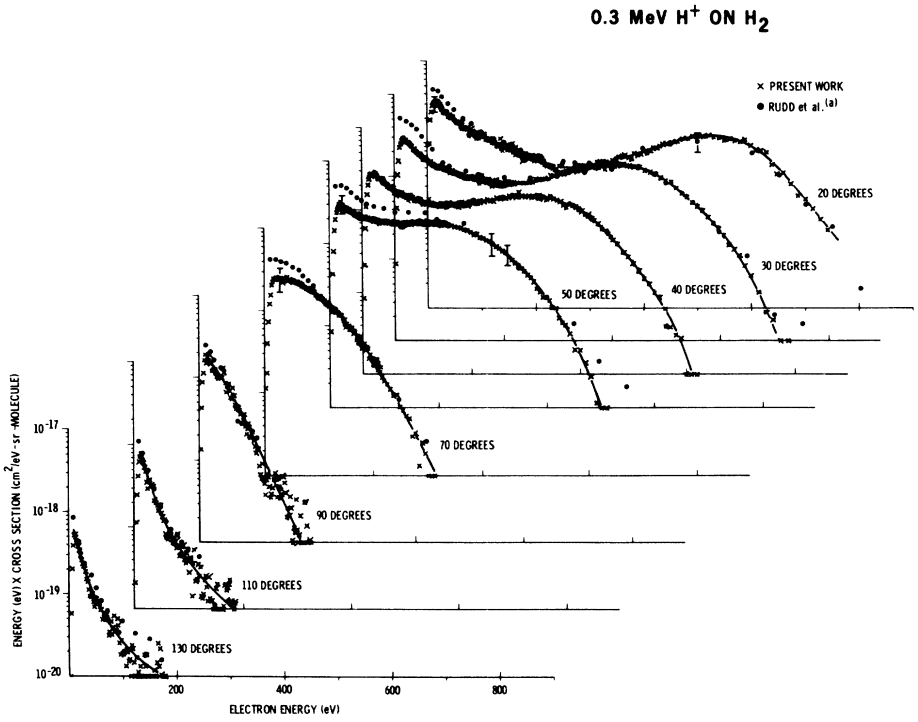

FIG. 5. Cross sections, differential in electron energy and angle of emission, for ejection of electrons by 0.3-MeV protons on molecular hydrogen. Previous measurements: (a) see Ref. 3.

trons with energies less than 100 eV at these angles, the measurements of Rudd *et al.*[3] result in cross sections as much as a factor of 2 larger than our results. These discrepancies are greater than the combined experimental uncertainties of the respective experiments which were estimated to be 30% by Rudd *et al.*[3] and evaluated as 25% in the present work. For very-low-energy electron emission, energies less than approximately 15 eV, our measured cross sections begin to decrease with decreasing energy, whereas the results of Rudd *et al.*[3] continued to increase until the electron energy was reduced to approximately 5 eV. We have attributed the decrease in our values at these low electron energies to a reduction in the transmission of the analyzer at low energies and to the effects of residual magnetic fields which are important at these very low electron energies. Both of these effects are considered negligible for electron energies greater than approximately 30 eV.

Cross sections, differential in electron energy only, are shown in Fig. 6 for 0.3-MeV protons on hydrogen. These cross sections were obtained by integrating those of Fig. 5 with respect to emission angle. Here, again, there is agreement within experimental uncertainties between the present results and the work of Rudd *et al.*[3] throughout most of the energy range of the ejected electrons. For electron energies near 350 eV, the results of Rudd *et al.* fall slightly below the present measurements. This is the energy region where the 40° spectrum shown in Fig. 5 exhibits a peak, and it is expected that the addition of data from a spectrum obtained at 40° into the angular integration of Rudd *et al.*[3] would bring his results into agreement with ours.

Error bars shown in the figures are representative of uncertainties in the cross sections due both to systematic uncertainties associated with calculation of the absolute values, and to random uncertainties resulting from statistical fluctuations encountered in data accumulation. The largest uncertainty in the cross sections results from the evaluation of the absolute value, approximately 25%, except for very small cross sections where the statistical fluctuations are quite large because

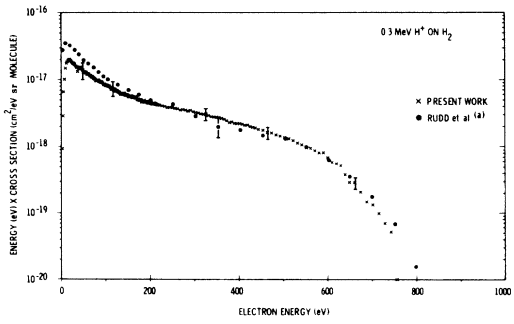

FIG. 6. Cross sections, differential in electron energy, for ejection of electrons by 0.3-MeV protons on hydrogen. Previous measurements: (a) see Ref. 3.

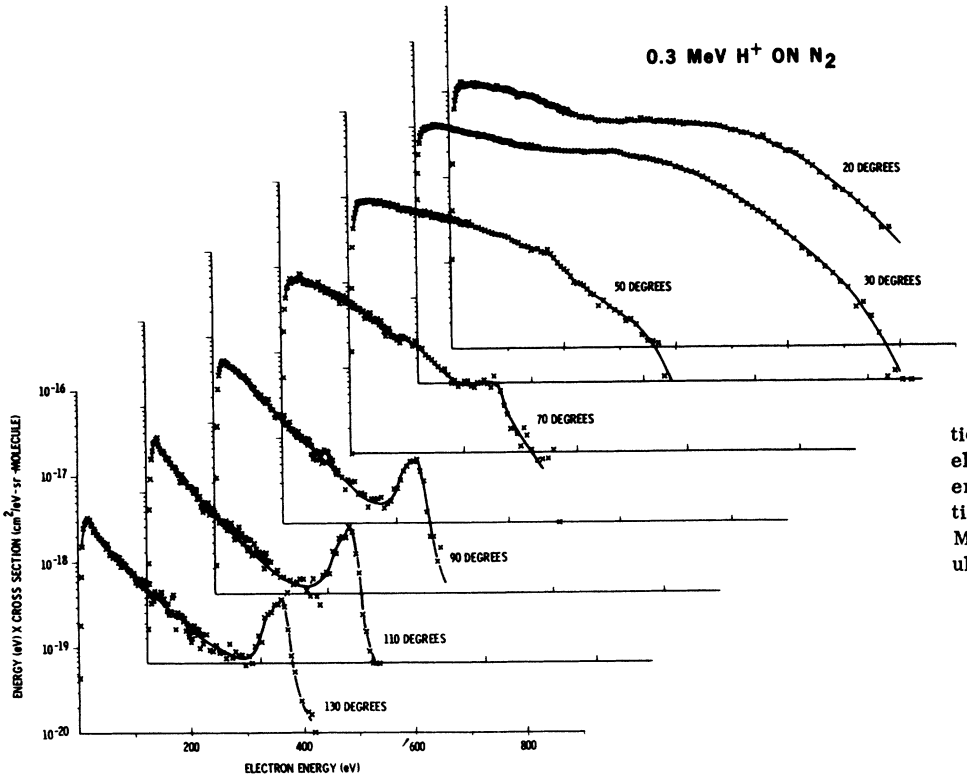

FIG. 7. Cross sections, differential in electron energy and emission angle, for ejection of electrons by 0.3-MeV protons on molecular nitrogen.

of low counting rates and uncertain background subtractions. The background count rate was due to electrons and photons which were scattered from the walls of the vacuum chamber, electrostatic analyzer, target cell, etc., and eventually reached the electron multiplier where they were counted. The magnitude of this background was evaluated from the count rate obtained when the potential on the electrostatic analyzer had been increased until it was no longer energetically possible to produce electrons by proton-electron collisions with sufficient energy to pass through the analyzer. In most cases, the background was negligible. For the very small cross sections where signal and background count rate became comparable, the total uncertainty in the cross section may be quite large, as is indicated in our results by the scatter of data points and representative error bars. The solid line drawn through the points is a best estimate of our measured cross sections.

Cross sections, differential in electron energy and emission angle, were measured for electron ejection from nitrogen gas under proton impact, and are shown in Figs. 7–11 for proton energies of 0.3, 0.5, 1.0, 1.4, and 1.7 MeV, respectively. The cross sections were measured for 7–10 different angles between 20° and 130° with respect to the forward direction of the proton beam. General features of the electron spectra include a maximum in the cross sections at very low electron energies with a gradual decrease for larger energies, a K Auger peak between approximately 300 and 400 eV, and a broad peak for electrons ejected at forward angles with energies corresponding to the kinematic maximum energy transfer. The peak due to K Auger emission has a maximum value at approximately 365 eV and corresponds to the $1s$-$2p2p$ Auger transition. The resolution of the electrostatic analyzer was not sufficient to resolve individual components of the K Auger group; however, group intensities were obtained and are discussed later.

The energies at which maxima occur in the high-energy region of the spectra for electrons ejected at forward angles are approximately equal to the maximum energies which can be transferred in a binary collision between the incident proton and a free electron. In Fig. 12, cross sections, differential in ejection energy and angle, are plotted as a function of emission angle for three ejected electron energies; the marker on each curve indicates the angle at which the maximum would be expected if the interaction were between a proton and free electron. A rather sharp maximum is observed for ejection of high-energy electrons (1000 eV) at angles corresponding to those predicted by the free-electron calculation, whereas the calculated angles at which the maximum energy transfer would occur for low-energy electron ejection are larger

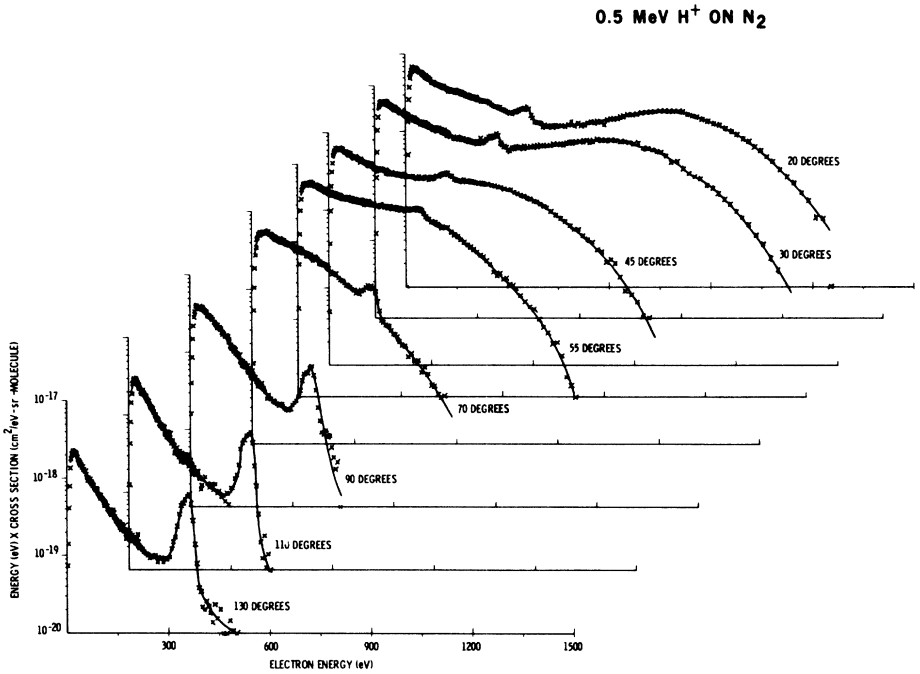

FIG. 8. Cross sections, differential in electron energy and emission angle, for ejections of electrons by 0.5-MeV protons on molecular nitrogen.

than were found experimentally. These discrepancies for low electron energies are to be expected as a consequence of the electron being bound to the nitrogen molecule. The general trend in the results as a function of electron energy is not notably affected by changes in the proton energy from 0.3 to 1.7 MeV. The fact that 0.3- and 1.7-MeV protons produce similar effects is not surprising since the 0.3-MeV protons are already moving with a velocity much greater than all but the most tightly bound electrons in the nitrogen molecule. For intermediate electron energies, such as represented by 250-eV electrons in Fig. 12, the forward peak is found at somewhat smaller angles than those given by the free-electron calculation, and there appears to be some evidence of an increase in the

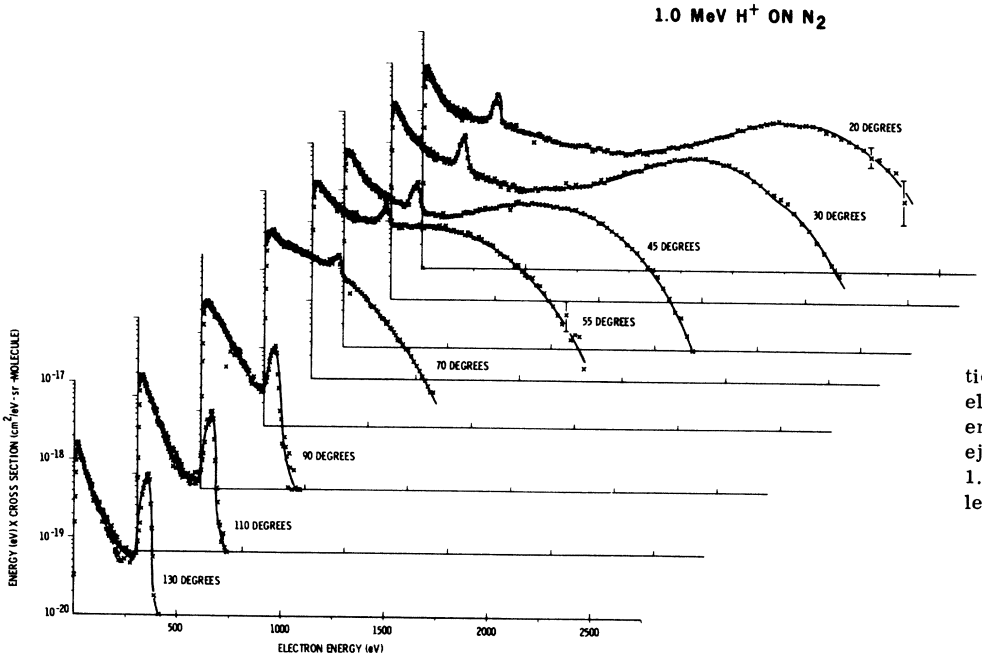

FIG. 9. Cross sections, differential in electron energy and emission angle, for ejection of electrons by 1.0-MeV protons on molecular nitrogen.

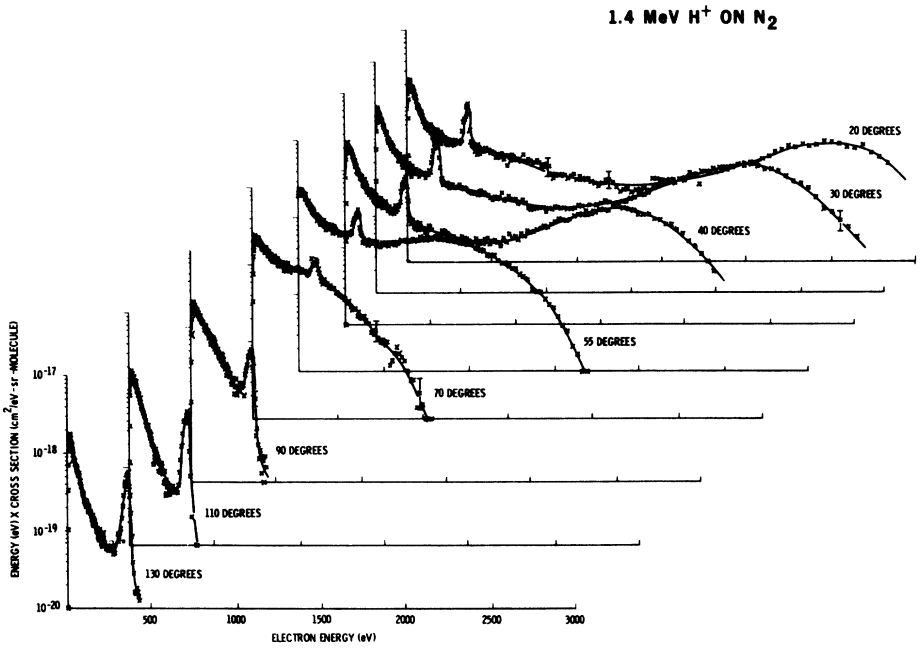

FIG. 10. Cross sections, differential in electron energy and emission angle, for ejection of electrons by 1.4-MeV protons on molecular nitrogen.

cross section in the backward direction. A more comprehensive series of curves presenting the angular dependence of cross sections for ejection of electrons of different energies is shown in Fig. 13 for 1.7-MeV protons on nitrogen. In this figure, there is also evidence of a peak in the emission cross section for backward scattering of electrons with energies of 150 and 250 eV. Similar peaks in the electron spectrum for backward angles have been observed by Rudd *et al.*[3] for low-energy protons on hydrogen and helium, by Ehrhardt *et al.*[15] for electrons on helium, and by Vroom[16] for electrons on nitrogen and argon. It is unfortunate that we were not able to position our analyzer at larger angles to verify whether there is actually a peak or whether we are observing a region at large emission angles where the cross sections are independent of emission angle. One might speculate that underlying the distribution from direct interactions there is an isotropic contribution due to

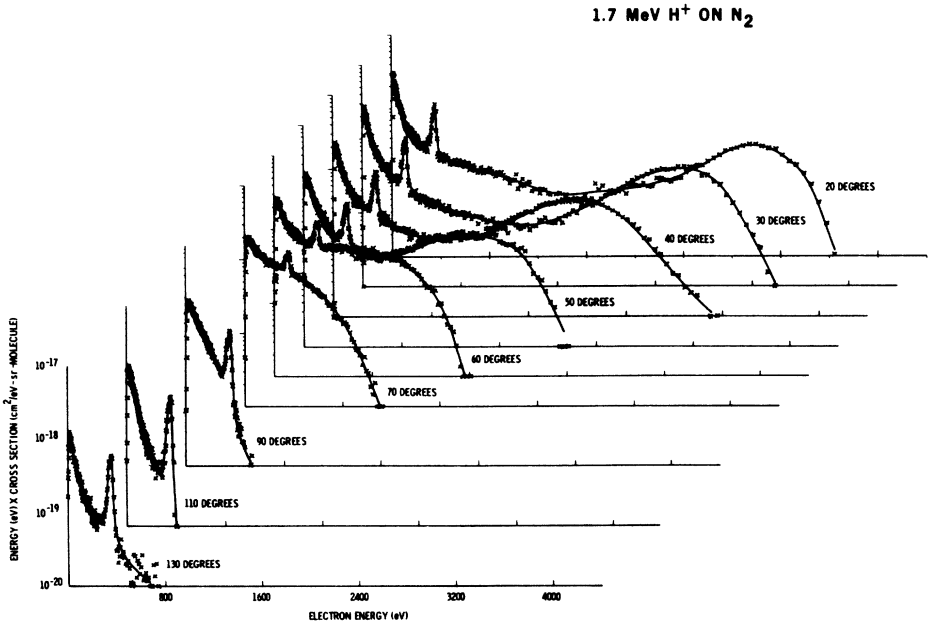

FIG. 11. Cross sections, differential in electron energy and emission angle, for ejection of electrons by 1.7-MeV protons on molecular nitrogen.

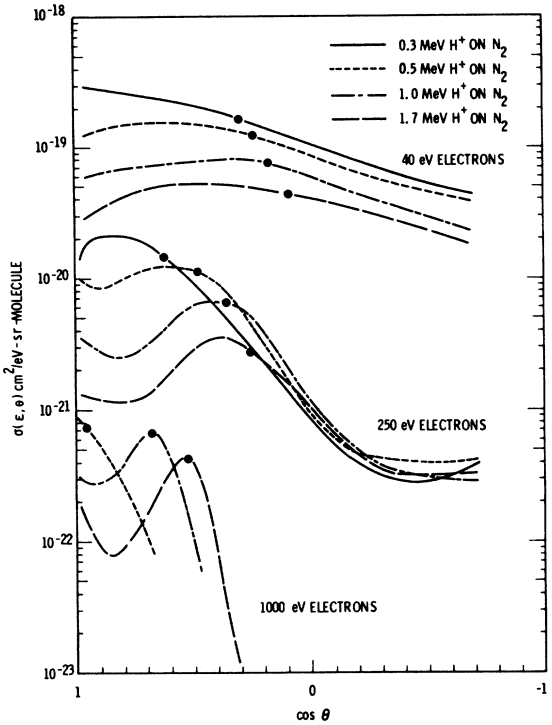

FIG. 12. Doubly differential cross sections plotted as a function of emission angle for selected electron energies and for several incident proton energies. The marker on each curve represents the position of an expected maximum based on a collision between the proton and a free electron.

Auger emission, which becomes evident at large angles, where the number of electrons due to direct interactions becomes small. However, for these electron energies, 150 and 250 eV, the Auger emission cross sections are smaller by an order of magnitude or more than the total cross sections plotted in Fig. 13. The dashed line cutting through the curves in Fig. 13 represents the angle at which maxima would be expected based on an interaction between the incident proton and a free electron. Again, as in Fig. 12, the approximate positions of these maxima are predicted quite well by the free-electron model for electron energies much greater than the binding energies. At present, there are no detailed calculations of doubly differential cross sections with which we can compare our results for high-energy protons on nitrogen gas.

Cross sections which are differential only in electron emission energy can be obtained from the measured cross sections by an integration with respect to the angle of electron ejection according to the following relationship:

$$\sigma(\epsilon) = 2\pi \int_0^{\pi} \sigma(\epsilon, \theta) \sin\theta \, d\theta \quad . \tag{2}$$

In order to integrate this expression using the measured doubly differential cross sections, the integral was approximated as follows:

$$\sigma(\epsilon) = 2\pi \left[\int_0^{\theta_1} \sigma(\epsilon, \theta) \sin\theta \, d\theta + \int_{\theta_1}^{\theta_2} \sigma(\epsilon, \theta) \sin\theta \, d\theta + \cdots + \int_{\theta_n}^{\pi} \sigma(\epsilon, \theta) \sin\theta \, d\theta \right] , \tag{3}$$

where n designates the total number of angles for which data were obtained and $\sigma(\epsilon, \theta)$ was assumed to have a linear dependence on θ between each set of angles. For the purposes of integration, values for $\sigma(\epsilon, \theta)$ at angles of 0 and π were taken to be the values measured at θ_1 and θ_n, respectively. This arbitrary evaluation of the cross sections at small and large angles does not influence the integrated cross section markedly because of the multiplicative factor $\sin\theta$ within the integral. The value of $\sigma(\epsilon)$ was also calculated for several electron energies by graphical integration with respect to angle in order to check the results of the method described above. When using this graphical method of integration, the angular dependence of $\sigma(\epsilon, \theta)$ could easily be varied from that obtained by the linear interpolation between measured cross sec-

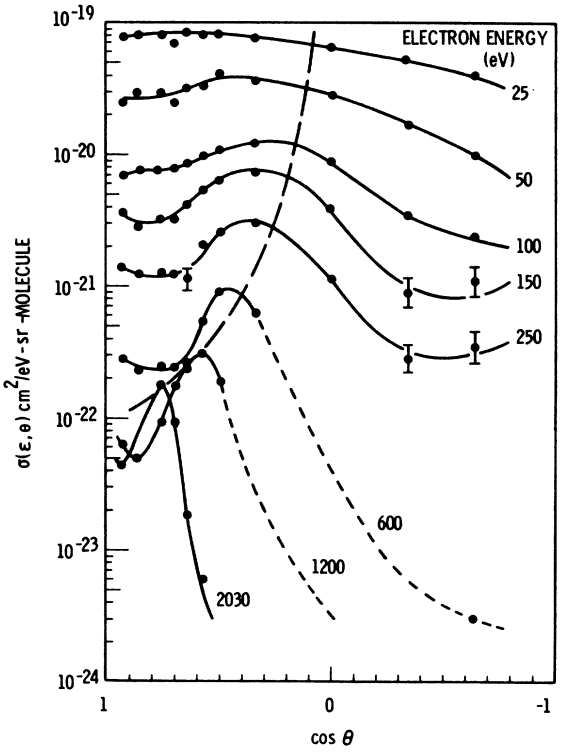

FIG. 13. Doubly differential cross sections for selected energies of the ejected electrons plotted as a function of emission angle for 1.7-MeV protons on nitrogen. The dashed line represents the position of an expected maximum based upon a collision between the proton and a free electron.

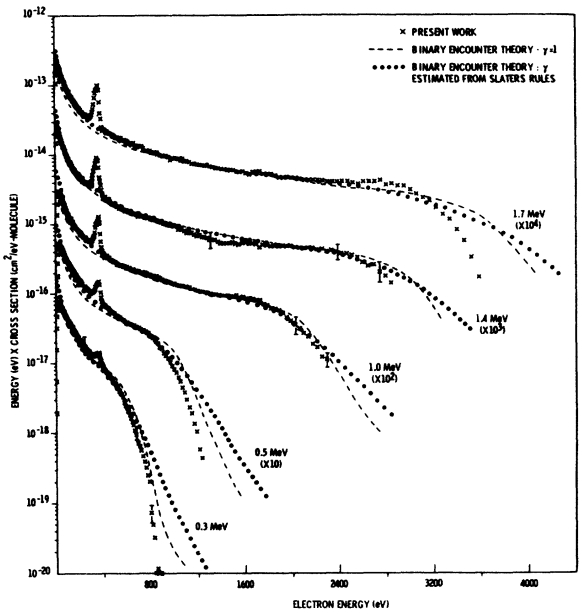

FIG. 14. Cross sections, differential in ejected electron energy, for incident protons with energies of 0.3, 0.5, 1.0, 1.4, and 1.7 MeV on nitrogen. The calculated results are from the program of Rudd and Gregoire (Ref. 17).

tions used in evaluating Eq. (3); and the uncertainty in the value of the integrated cross section due to the use of this linear interpolation could be estimated. Reasonable variations in the angular dependence and in the values of $\sigma(\epsilon, \theta)$ at both $\theta = 0$ and $\theta = \pi$ were found to produce changes in the integrated cross section of less than a few percent. The total uncertainty in the integrated cross sections, shown in Fig. 14, is expected to be 25% except at high electron energies where counting rates were quite low. The last few cross sections at the high-energy extreme of each spectrum were deduced from raw data in which the count rate of ejected electrons was comparable to the background count rate. These measured cross sections are, therefore, uncertain by as much as a factor of 2. The representative error bars shown in Fig. 14 are indicative of the total uncertainty in the integrated cross sections with confidence limits of 1 standard deviation.

The theoretical results shown in Fig. 14 were obtained from a program supplied by Rudd[17] which utilizes binary encounter theory based on the Gerjuoy-Vriens equations.[18,19] This is a semiclassical treatment in which the cross sections for electron ejection are calculated taking into account the relative velocity between the incident proton and the bound electron. The velocity distribution of the bound electrons is assumed to be isotropic with a quantum-mechanical speed distribution deduced from a Fock distribution. Other parameters in the calculation include the ionization potential of each atomic shell or subshell and the ratio γ of the orbital kinetic energy to the ionization potential. In Fig. 14, the results of two binary-encounter calculations are shown; in one calculation, the orbital kinetic energy was taken equal to the ionization potential $\gamma = 1$ and in the second, the orbital kinetic energy was estimated by Slater's rules[20] applied to atomic nitrogen. Partial cross sections were calculated for electron ejection from each electronic shell; these results were then weighted according to the number of electrons in each shell and summed to give emission cross-sections differential only in electron energy. The molecular properties of nitrogen enter into the calculation only to the extent that the molecular ionization potential was used for the outer shell electrons. The results, shown in Fig. 14, indicate that the choice of γ makes very little difference in the calculated cross sections throughout most of the energy range of both the ejected electrons and the incident protons. Discrepancies which do exist between the cross sections calculated using the two values of γ occur at the low- and high-energy extremes of the electron spectra. It is not clear from a comparison with measured cross sections which values of γ lead to the most accurate cross sections, since $\gamma = 1$ results in cross sections which agree best for high-energy electron ejection, and the determination of γ by application of Slater's rules brings about the best agreement for low-energy electrons. In general, the binary-encounter calculations and the measured cross-sections differential in electron energy agree to within a factor of 2, and over most of the energy range of the ejected electrons the agreement is within the experimental uncertainties assigned to the measured cross sections. Binary-encounter theory does not, of course, predict any structure in the electron spectra such as the K Auger peaks except by inference, in that the Auger transitions are a consequence of filling K-shell vacancies which are predicted by the theory.

One can obtain the total cross section for K Auger emission from the cross-sections differential in electron energy, shown in Fig. 14, by integration with respect to energy of the K Auger peaks after subtraction of the contribution due to direct interactions. The part of the total cross sections caused by direct interactions between the incident proton and bound electron can be estimated in the region of the spectrum under the K Auger peaks by fitting an exponential curve to the measured cross sections at energies above and below the energy range of the Auger transitions. A representative plot of the cross sections for K Auger emission, differential in electron energy, is shown in Fig. 15 for 1.0-MeV proton impact. As noted previously, the

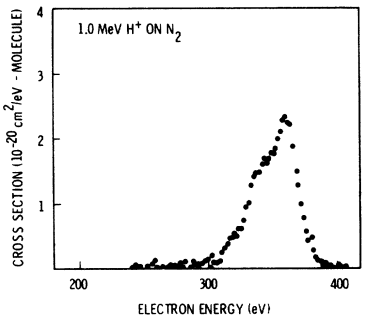

FIG. 15. Cross section for K Auger emission, differential in electron energy, from 1.0-MeV proton impact on nitrogen.

resolution of our electrostatic analyzer (5.5%) was not sufficient to resolve structure in the K Auger electron group. However, the cross sections for total K Auger emission obtained by integration of cross sections such as those shown in Fig. 15 provided an estimation of the K-shell ionization cross sections. Since the fluorescence yield for nitrogen is less than 1%, [21] each K-shell vacancy may be considered to be filled by an outer shell electron with the subsequent emission of a K Auger electron, and the total cross section for K Auger emission is approximately equal to the cross section for K-shell ionization. A deviation from the one K Auger electron per K-shell vacancy can result from double Auger emission. In this process, two electrons are ejected with a third electron filling the original K-shell vacancy. Carlson and Krause[12] have shown that the spectrum of one of the two ejected electrons will have its maximum value at an electron energy equal to the K-shell binding energy minus the binding energy of the two electrons which are ejected and the electron which fills the K vacancy (approximately 330 eV for nitrogen), whereas the spectrum of the other ejected electron will have its maximum value for near zero electron energy. Since our K Auger group intensity is obtained by integrating a limited energy region (240–420 eV) only one of the two electrons ejected in double Auger emission will be detected, thus retaining the validity of our assumption of one K Auger electron per one K vacancy. Thus, the accuracy with which one can determine K-shell ionization cross sections by this method depends primarily upon the accuracy of the total cross sections for electron emission and upon the accuracy of the subtraction of the contribution due to direct interactions. In the present work, the uncertainties in the K-shell ionization cross sections are estimated to be 25%, except for the 0.3-MeV proton impact, where the uncertainty in the subtraction of the direct interaction contribution for this relatively small K Auger intensity results in a 50% uncertainty in the K-shell ionization cross section. The results of these measurements are shown in Fig. 16 where the error bars represent confidence limits of 1 standard deviation. The binary-encounter results shown in Fig. 16 were obtained by integration with respect to emission energy of the cross section for electron ejection from the K shell of nitrogen by proton impact. The program of Rudd and Gregoire[17] was used for this calculation with the ratio of orbital kinetic energy to binding energy γ deduced from Slater's rules[20] applied to atomic nitrogen. If the value of γ for each atomic shell were taken to be one in this calculation, the resulting cross sections would be increased by less than 10%. If one estimates the K-shell ionization cross sections by an extrapolation of the work of Mertzbacher and Lewis[22] to atomic number 7, the estimated values are a factor of 2 to 3 smaller than measured. This discrepancy is not surprising, however, since their work was not meant to apply to target atoms with atomic numbers this low.

V. SUMMARY

The agreement between the present measurements and cross sections calculated from binary-encounter theory is quite good for both the K-shell ionization cross sections and the electron emission cross-sections differential in electron energy. In the regions of the electron-energy spectra where discrepancies do exist, these differences between measured and calculated cross sections are less than a factor of 2 with the exception of the extreme high- and low-energy ends of the spectra where experimental uncertainties are very large. A more sensitive test of the theory would be a comparison with the measured angular distributions; however, at this time these calculations are not available.

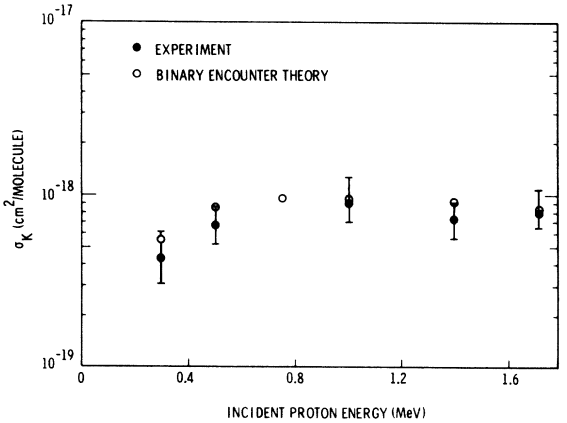

FIG. 16. K-shell ionization cross sections for proton impact on nitrogen. The cross sections calculated by binary-encounter theory were obtained from the program of Rudd and Gregoire (Ref. 17).

ACKNOWLEDGMENTS

The author would like to thank W. A. Glass for suggesting this research and for his helpful comments throughout the investigation. The help of L. A. Braby on the initial design and construction of the apparatus is appreciated. He is indebted to W. C. Roesch for writing the computer programs for the solid-angle calculations and to W. C. Roesch and W. E. Wilson for many valuable discussions throughout this research and in preparation of this paper. The author would also like to thank A. K. Edwards for sending drawings of his electrostatic analyzer from which ours was designed and M. E. Rudd for providing a copy of his computer program for the binary-encounter calculations.

*Paper based on work performed under U. S. Atomic Energy Commission Contract No. AT(45-1)-1830.

[1]C. E. Kuyatt and T. Jorgensen, Jr., Phys. Rev. 130, 1444 (1963).

[2]M. E. Rudd and T. Jorgensen, Jr., Phys. Rev. 131, 666 (1963).

[3]M. E. Rudd, C. A. Sautter, and C. L. Bailey, Phys. Rev. 151, 20 (1966).

[4]H. Hafner, J. Arol Simpson, and C. E. Kuyatt, Rev. Sci. Instr. 39, 33 (1968).

[5]V. V. Zashkvara, M. I. Korsunskii, and O. S. Kosmachev, Zh. Tekh. Fiz. 36, 132 (1966) [Soviet Phys. Tech. Phys. 11, 96 (1966)].

[6]H. Z. Sar-el, Rev. Sci. Instr. 38, 1210 (1967).

[7]A. Egidi, R. Marconero, G. Pizzella, and F. Sperli, Rev. Sci. Instr. 40, 88 (1969).

[8]K. C. Schmidt, Bendix Electro-Optics Division Technical Applications Note 9803, 1969 (unpublished).

[9]S. Dushman, *Scientific Foundations of Vacuum Techniques* (Wiley, New York, 1962).

[10]E. Bar-Avraham and L. C. Lee, University of Southern California Report No. USC-136-138, 1968 (unpublished).

[11]C. E. Normand, Phys. Rev. 35, 1217 (1930).

[12]T. A. Carlson and M. O. Krause, Phys. Rev. Letters 17, 1079 (1966).

[13]A. K. Edwards and M. E. Rudd, Phys. Rev. 170, 140 (1968).

[14]Tabulated cross sections can be obtained from the author upon request.

[15]H. Ehrhardt, M. Schulz, T. Tekaat, and K. Willmann, Phys. Rev. Letters 22, 89 (1969).

[16]D. A. Vroom, Gulf General Atomic Annual Report No. GA 9713, UC-34, 1969 (unpublished).

[17]M. E. Rudd and D. Gregoire, in *Physics of the One- and Two-Electron Atoms*, edited by F. Bopp and H. Kleinpoppen (North-Holland, Amsterdam, 1969), pp. 795–800; M. E. Rudd (private communication).

[18]E. Gerjuoy, Phys. Rev. 148, 54 (1966).

[19]L. Vriens, Proc. Phys. Soc. (London) 90, 935 (1967).

[20]B. B. Robinson, Phys. Rev. 140, A764 (1965).

[21]E. J. McGuire, Phys. Rev. 185, 1 (1969).

[22]E. Mertzbacher and H. W. Lewis, in *Encyclopedia of Physics*, edited by S. Flügge (Springer-Verlag, Berlin, 1958), Vol. 34, pp. 166–192.

PHYSICAL REVIEW A VOLUME 3, NUMBER 1 JANUARY 1971

Absolute Excitation Cross Sections of He^+ in 20-100-keV He^+-He Collisions Using Energy-Loss Spectrometry*

D. R. Schoonover† and John T. Park
Physics Department, University of Missouri, Rolla, Missouri 65401
(Received 30 July 1970)

Application of positive-ion energy-loss spectrometry has been extended to include experimental determination of absolute excitation cross sections of ground-state helium ions. Helium ion-atom collisions were studied for impact energies ranging between 20–100 keV, in 10-keV intervals. The data were taken with an apparatus resolution between 0.6–0.8 eV full width at half-maximum (FWHM). Cross sections for transitions from ground state to the second and third principal quantum levels of the ion plotted as a function of impact energy were still rapidly increasing at 100 keV. The cross sections at this energy were $(1.64 \pm 0.28) \times 10^{-18}$ cm^2 for $He^+(1^2s_{1/2}) \rightarrow He^+ (n=2)$ and $(3.46 \pm 0.45) \times 10^{-19}$ cm^2 for $He^+ (1^2s_{1/2}) \rightarrow He^+ (n=3)$.

I. INTRODUCTION

The technique of energy-loss spectrometry is rapidly becoming a major tool for studying elementary collision processes. In electron spectrometry, electron exchange and target transitions can be studied. In positive-ion energy-loss spectrometry, excitation of the projectile ion can also occur. The relative velocity of approach (rather than the impact energy) is the primary parameter considered when making approximations in theoretical calculations.[1] Therefore, since positive ions are considerably

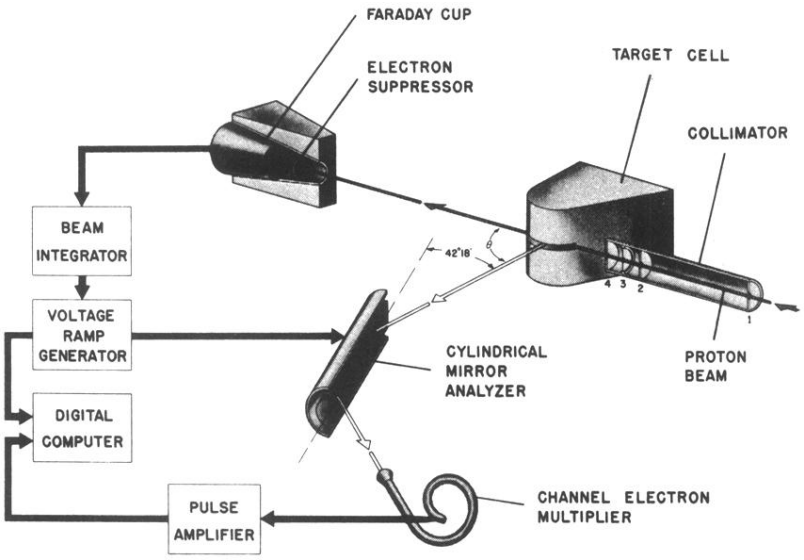

FIG. 1. Schematic drawing of the apparatus used for the cross-section measurements.